Classical-trajectory Monte Carlo model calculations for the antiproton-induced ionization of atomic hydrogen at low impact energy

L. Sarkadi* and L. Gulyás

Institute for Nuclear Research of the Hungarian Academy of Sciences (ATOMKI), H-4001 Debrecen, Pf. 51, Hungary

(Received 9 May 2014; revised manuscript received 9 July 2014; published 8 August 2014)

The three-body dynamics of the ionization of the atomic hydrogen by 30-keV antiproton impact has been investigated by calculation of fully differential cross sections (FDCSs) using the classical-trajectory Monte Carlo (CTMC) method. The results of the calculations are compared with the predictions of quantum mechanical descriptions: The semiclassical time-dependent close-coupling theory; the fully quantal, time-independent close-coupling theory; and the continuum-distorted-wave-eikonal-initial-state model. In the analysis particular emphasis was put on the role of the nucleus-nucleus (NN) interaction played in the ionization process. For low-energy electron ejection the CTMC method predicts a large NN interaction effect on FDCSs, in agreement with the quantum mechanical descriptions. By examining individual particle trajectories it was found that the relative motion between the electron and the nuclei is coupled very weakly with that between the nuclei, consequently the two motions can be treated independently. A simple procedure is presented by which the NN interaction effect can be included in the calculations carried out without it.

DOI: 10.1103/PhysRevA.90.022702 PACS number(s): 34.50.Fa, 34.10.+x

I. INTRODUCTION

The ionization of the hydrogen atom by impact of antiprotons has attracted the attention of many theoreticians in the past decades. The great interest is explained by the fact that in the treatment of the process one is faced with a clean three-body breakup problem: In contrast to proton impact there is no electron capture channel, and unlike the electron-induced ionization, the treatment is not complicated by electron exchange effects.

The enormous efforts devoted to the investigations of the collisions of antiprotons with atoms and molecules have been reviewed recently [1]. Besides the fundamental aspects of the topic, from the review the reader may learn about important, potential applications, for example, the radiation therapy for cancer treatment. Although the dominant process utilized in the therapy is the annihilation, there are several aspects of atomic physics relevance of this application, e.g., the slowing down process of the antiprotons in the biological issue and the mechanism of creation of slow secondary electrons.

The subject of most of the research work carried out on the antiproton-induced ionization of the hydrogen atom was the energy-dependent total cross section. The small number of differential studies is explained partly by the present experimental limitations (first of all, the small intensity of the available antiproton beam), and theoretically the difficulties arising in the calculations of accurate partially or fully differential cross sections.

The deepest insight into the dynamics of the collision can be gained by kinematically complete experiments. A technique used widely for this purpose in the field of atomic collisions is COLTRIMS (cold-target-recoil-ion-momentum spectroscopy) [2]. COLTRIMS was applied in the only experimental study in which differential cross sections were measured for collisions involving antiprotons [3]. In the experiment carried out for helium targets at 945-keV impact energy, the differential cross sections in the longitudinal electron and recoil-ion momenta were determined. The obtained data showed only a small (<10%) difference from the corresponding cross sections measured by 1-MeV protons, as is expected at such high impact energy.

The above experiment demonstrated the feasibility of differential measurements using antiprotons. This and future plans of facilities providing low-energy antiproton beams of high intensity (for a review see Ref. [4]) have given great momentum to the theoretical investigations of the differential properties of the antiproton-induced ionization. Another motivation towards this direction was the clarification of the effect of nucleus-nucleus (NN) interaction on the fully differential cross sections (FDCSs) in ion-atom collisions. The role of the NN interaction was one of the central questions of the attempts to solve the long-standing puzzle regarding discrepancies between theory and experiment in the FDCSs for ionization in 100 MeV/amu C^{6+} + He collisions [5] (for a review see, e.g., Ref. [6]). The effect of the NN interaction on the ionization depends on the sign of the projectile charge; therefore it is expected to contribute to the particle-antiparticle differences in FDCSs.

Exhaustive reviews of the available theoretical differential studies of the antiproton-induced ionization of hydrogen have been given in recent papers by Abdurakhmanov *et al.* [7] and Ciappina *et al.* [8]. In the following we briefly summarize the models applied for calculation of FDCSs. In most of the works the authors compare the results of their calculations with the predictions of the first Born approximations (FBA). Further, fully quantum mechanical first-order perturbation approaches that include the NN interaction are the continuum-distorted-wave–eikonal-initial-state (CDW-EIS) model of Voitkiv and Ullrich [9], that of Jones and Madison [10], and the three-Coulomb-wave (3C) model of Berakdar *et al.* [11]. Voitkiv and Ullrich [9] have also made calculations in the second-order Born approximation.

Nonperturbative descriptions have also been applied in fully differential studies. McGovern *et al.* [12–14] worked out a model within the framework of a time-dependent

*sarkadil@atomki.hu

coupled pseudostate (CP) formalism. Although they used the straight-line approximation (SLA) for the projectile path, they could determine FDCSs by establishing connection between the wave treatment of projectile motion and the SLA method. In this way their model gives account of the NN interaction. The fully quantal, time-independent convergent close-coupling (CCC) model of Abdurakhmanov *et al.* [7] has been developed along the lines of the CCC approach to electron-atom scattering. The model is also based on use of pseudostates, and as a fully quantal theory, it implicitly considers the NN interaction. Recently Ciappina *et al.* [8] investigated the differential properties of the antiproton-induced ionization within the framework of time-dependent close-coupling (TDCC) theory using SLA for the projectile path. They employed a Fourier transform method in order to extract the FDCS for a specific value of projectile momentum transfer and included the NN interaction into the model by a phase factor [15,16] in the Fourier integral of the transition amplitude over the impact parameter. For the sake of completeness we mention that further investigations using semiclassical coupled-channel approaches [17–20] have also been reported in the literature, but in these works only partially differential cross sections were calculated or some special aspects of the antiproton-hydrogen collision were analyzed.

In this paper we report the results of an analysis carried out by the classical-trajectory Monte Carlo (CTMC) method. The motivation for the work was as follows. From the comparison of the FDCSs predicted by the above models it turned out that there exist large discrepancies (more than factor of 2) between the models, particularly at low impact energies ($\leqslant$200 keV) [7,8]. The reason for the discrepancies can be traced back to the approximations applied in the models. Most importantly, for the electronic wave function all the models use *single-center* expansion based on the target atom. The reasoning for this approximation is that the antiproton has no bound states of electrons, and therefore in the lack of the electron capture channel there is no need to include projectile-centered states in the expansion of the wave function. However, at low impact velocities a large distortion of the electron distribution—a strong reduction of the electron density near the antiproton—is expected which cannot be represented by the one-center expansion, as was shown by Toshima [21]. Probably, as a consequence of the one-center approximation, in studies made with pseudostates the calculations were not repeated for protons, and therefore the analysis of one of the most interesting characteristics of the future antiproton experiments, the particle-antiparticle difference in FDCSs, is missing in these studies.

The CTMC method provides an exact description of the full dynamics of the three-body breakup process, albeit classically. It is known to reproduce the main features of the excitation, ionization, and charge transfer processes in ion-atom collisions. It can be successfully used for calculations of differential cross sections (as an example, see Ref. [22]). A further advantage of the CTMC method is that by analysis of the calculated trajectories one can gain a deeper insight into the dynamics of the collision processes. At the same time the model character of the method should be emphasized: Because of the neglect of quantum mechanical effects the CTMC method has a limited validity; in a number of applications it proved to be only a qualitative description. For example, for proton on hydrogen collisions the CTMC method underestimates the total ionization cross section at 20-keV impact energy by more than a factor of 2, and even at higher proton energies it fails to reproduce the observed angular distribution of the ejected electrons at backward angles [23].

We made the CTMC calculations at a relatively low impact energy of 30 keV where large particle-antiparticle differences in FDCS are expected. Another reason for the choice of 30 keV was that at this energy FDCS calculations were performed in most of the quantum mechanical models, providing a basis for the comparison of the various approaches. We note that the number of studies applying the CTMC method to study the full three-body dynamics in ion-atom collisions is very scarce [24,25]. At the same time, the CTMC method has been applied in several works [3,26–28] to calculate partially differential cross sections for the antiproton-induced ionization of the helium atom.

II. THEORETICAL METHOD

The CTMC method is based on the numerical solution of the classical equations of motion for a large number of trajectories of the interacting particles under randomly chosen initial conditions [29,30]. The details of the CTMC computer code used are given in Ref. [31]. Briefly, it solves Newton's nonrelativistic equations of motion for the three particles (in atomic units):

$$m_i \frac{d^2\mathbf{r}_i}{dt^2} = \sum_{j(\neq i)=1}^{3} Z_i Z_j \frac{\mathbf{r}_i - \mathbf{r}_j}{|\mathbf{r}_i - \mathbf{r}_j|^3}, \quad (i = 1,2,3). \qquad (1)$$

Here m_i, Z_i, and $\mathbf{r}_i$ are the masses, charges, and position vectors of the particles, respectively. The randomly selected initial conditions were the impact parameter and five further parameters defining the position and velocity vector of the target electron moving on Kepler orbits. The ranges of the latter parameters were constrained to give the binding energy of the hydrogen atom, 0.5 a.u. For the generation of the initial values of the position and velocity coordinates of the electron from a set of uniformly distributed variables we applied the general procedure suggested by Reinhold and Falcón [32] for non-Coulombic systems, which is equivalent to the original Abrines and Percival's method [29] in the case of the Coulomb interaction.

The integration of the equations of motion was started at a large distance (138 a.u.) between the incoming projectile and the hydrogen atom. After the collision the calculations were made in two steps. In the first step the integration was continued until the internuclear distance $R = 138$ a.u., where the main reaction channels (excitation, ionization, and charge transfer for proton impact) could be identified safely. In the second step only collision events leading to ionization were regarded. For the accurate determination of the postcollisional effects on the electron emission [33,34], in the second step the trajectories of the particles were calculated up to $R = 10^8$ a.u.

The fully differential cross section for ejection of the electron with energy between E_e and $E_e + dE_e$ into solid angle $d\Omega_e$ and for scattering of the projectile into solid angle

$d\Omega_p$ is expressed classically as

$$\frac{d^3\sigma}{dE_e d\Omega_e d\Omega_p} = 2\pi \int_0^\infty b \frac{d^3P}{dE_e d\Omega_e d\Omega_p}(b) db, \qquad (2)$$

where $d^3P/dE_e d\Omega_e d\Omega_p$ is the fully differential ionization probability of the process, and b is the impact parameter. One can easily show that for a large number N of collision events characterized by uniformly distributed b values in the range $(0, b_{\max})$ the integral in Eq. (2) can be approximated by the following sum:

$$\int_0^\infty b \frac{d^3P}{dE_e d\Omega_e d\Omega_p}(b) db \approx \frac{b_{\max} \Sigma_j b_j^{(i)}}{N \Delta E_e \, \Delta\Omega_e \, \Delta\Omega_p}. \qquad (3)$$

Here $b_j^{(i)}$ is the actual impact parameter at which the electron is emitted into energy and solid angle window ΔE_e and $\Delta\Omega_e$, and the projectile is scattered into solid angle window $\Delta\Omega_p$. The solid angles $\Delta\Omega_k$ $(k = e, p)$ are determined by the minimum and maximum values of the respective polar and azimuthal angles, θ_k and ϕ_k:

$$\begin{aligned}\Delta\Omega_k &= \int_{\theta_k^{\min}}^{\theta_k^{\max}} \int_{\phi_k^{\min}}^{\phi_k^{\max}} \sin\theta_k \, d\theta_k \, d\phi_k \\ &= \left(\cos\theta_k^{\min} - \cos\theta_k^{\max}\right)\left(\phi_k^{\max} - \phi_k^{\min}\right). \qquad (4)\end{aligned}$$

In our calculations we followed the history of 8×10^7 (1.6×10^8) collision events with $b_{\max} = 3.5$ (5) a.u. for antiproton (proton) impact. We carried out two series of calculations: We repeated the computer runs for the same collision events also without the NN interaction.

III. RESULTS AND DISCUSSION

For the total cross section of the ionization of the hydrogen atom by impact of 30-keV antiprotons the CTMC method resulted in 1.30×10^{-16} cm^2, which agrees with the measured value of $(1.14 \pm 0.25) \times 10^{-16}$ cm^2 [1,35] within the experimental error. At the same time, the corresponding value of 0.76×10^{-16} cm^2 for proton impact is smaller by 35% than the measured value of $(1.18 \pm 0.026) \times 10^{-16}$ cm^2 [36]. We note that in the lack of experimental data exactly at 30 keV, we obtained the above cross-section values by extrapolating and interpolating the published data for the antiproton and proton impact, respectively. As far as the NN interaction is concerned, it has a negligible (<1%) effect on the calculated total cross sections for both projectiles.

From the results of the computer runs we derived FDCS values at electron energy $E_e = (5 \pm 1)$ eV and projectile scattering angle $\theta_p = (0.35 \pm 0.05)$ mrad in the laboratory reference system. The latter value corresponds to an average transverse momentum transfer $q_\perp = 0.7$ a.u. We considered coplanar collision geometry; i.e., electron emission events occurring in the collision plane were selected. The latter plane is defined by the initial and final momentum of the projectile, $\mathbf{K}_i$ and $\mathbf{K}_f$, respectively. The condition of the coplanar electron emission was fulfilled by the choice $\phi_e - \phi_p = 0^\circ \pm 5^\circ$. The above choice of the collisional parameters means that for calculation of FDCSs in Eq. (3) we used $\Delta E_e = 2$ eV, $\Delta\theta_p = 0.1$ mrad, and $\Delta\phi_e = 10^\circ$. The azimuthally isotropic scattering of the projectile was expressed by taking $\Delta\phi_p = 2\pi$.

We mention here the main difficulty in the calculation of FDCSs using a Monte Carlo method, namely, that the specification of the kinematical parameters of the collision by sufficiently narrow windows strongly reduces the number of the regarded ionization events, and to achieve a reasonable counting statistics one needs to follow the history of a very large number of collisions.

The results of the calculations for antiproton and proton impact are presented in Figs. 1 and 2, respectively. In the figures we plotted also the prediction of FBA. The latter cross section can be expressed analytically (see, e.g., Ref. [12]). In the laboratory frame (in atomic units),

$$\begin{aligned}\frac{d^3\sigma}{dE_e d\Omega_e d\Omega_p} = &\frac{256 Z_p^2 m_p^2 v_f}{v_0 q^2 \pi [1 - \exp(-2\pi/\kappa)]} \\ &\times \frac{\exp\left[-\frac{2}{\kappa}\arctan\left(\frac{2\kappa}{1+q^2-\kappa^2}\right)\right]}{(1+q^2-\kappa^2)^2 + 4\kappa^2} \\ &\times \frac{q^2 - 2\boldsymbol{\kappa}\mathbf{q} + \frac{(\kappa^2+1)}{\kappa^2 q^2}(\boldsymbol{\kappa}\mathbf{q})^2}{(1+q^2+\kappa^2-2\boldsymbol{\kappa}\mathbf{q})^4}. \qquad (5)\end{aligned}$$

Here v_0 (v_f) is the initial (final) velocity of the projectile. $\boldsymbol{\kappa}$ is the momentum vector of the ejected electron, and $\mathbf{q} = \mathbf{K}_i - \mathbf{K}_f$ is the momentum transfer vector. We note that the sign of the terms $2\boldsymbol{\kappa}\mathbf{q}$ in Eq. (5) differs from that in Eq. (77) of Ref. [12], but agrees with that in Eq. (7.2.31) of Ref. [37].

In a naive view of the ionization the electron is expected to fly out from the atom in the direction of the transferred momentum due to the dominant electron-projectile interaction, i.e., the angular distribution of the electron is expected to be peaked at $\theta_e = \theta_q$ (at the present collisional parameters $\theta_q = 48^\circ$). This explains why the FDCS is plotted against the relative electron emission angle $\theta_e - \theta_q$ in Figs. 1(a) and 2(a). In panel (b) of the figures we plotted also the dependence of the FDCS on θ_e in the form of a polar diagram. In the latter diagram the emphasis was put on the directional information; therefore the distributions were normalized at their maximum values.

As is seen from the figures, the FBA predicts forward electron emission in the direction of the momentum transfer, in accordance with the aforementioned expectation. This can be understood considering that the FBA accounts only for the projectile-electron interaction. Furthermore, the FBA yields equal FDCSs for antproton and proton impact because of the Z_p^2 dependence on the projectile charge.

The FBA peak in Figs. 1 and 2 is the result of a direct momentum transfer in the binary collision between the projectile and the electron; therefore it is called the "binary peak." Under suitable collision conditions (higher collision velocity and lower projectile scattering angle) a second structure (called the "recoil peak") also appears in the angular distribution. It has a maximum in the direction of $-\mathbf{q}$, and it is interpreted as a double scattering process: First the electron is ejected via binary interaction with the projectile with momentum $\mathbf{q}$, then on its way out of the atom it backscatters elastically from the target nucleus (see, e.g., Ref. [5]).

For both projectiles the present CTMC calculations resulted in electron emission into completely different direction than that predicted by the FBA. First we discuss the case of

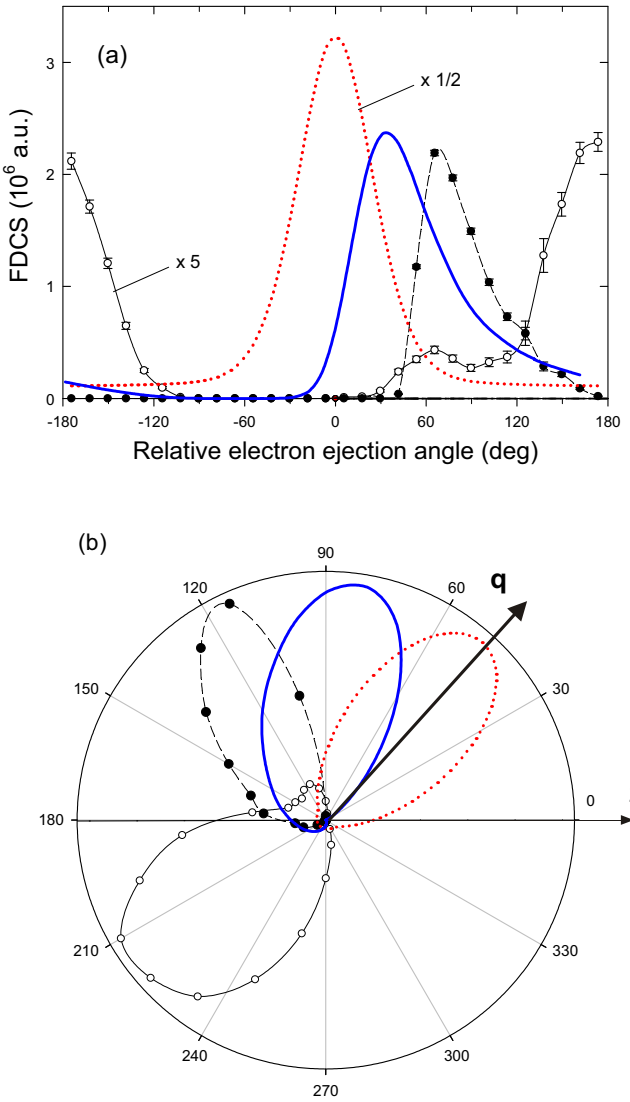

FIG. 1. (Color online) FDCS for ionization of the hydrogen atom by impact of 30-keV antiprotons in the scattering plane. The energy of the ejected electron is 5 eV; the scattering angle of the projectile is 0.35 mrad. Open circles, CTMC including the NN interaction; solid circles, CTMC neglecting the NN interaction; thick solid line (blue), CDW neglecting the NN interaction; dotted line (red), FBA. (a) The angular distribution of the electron as a function of the difference between the electron ejection angle θ_e and the direction of the momentum transfer vector θ_q. (b) Polar diagram of the electron electron emission as a function of the electron ejection angle θ_e. The distributions in the polar diagram are normalized at their maximum values. The arrow labeled q shows the direction of the momentum transfer. The z axis defines the direction of the incoming projectile beam. The thin solid and dashed lines through the CTMC results are only to guide the eye.

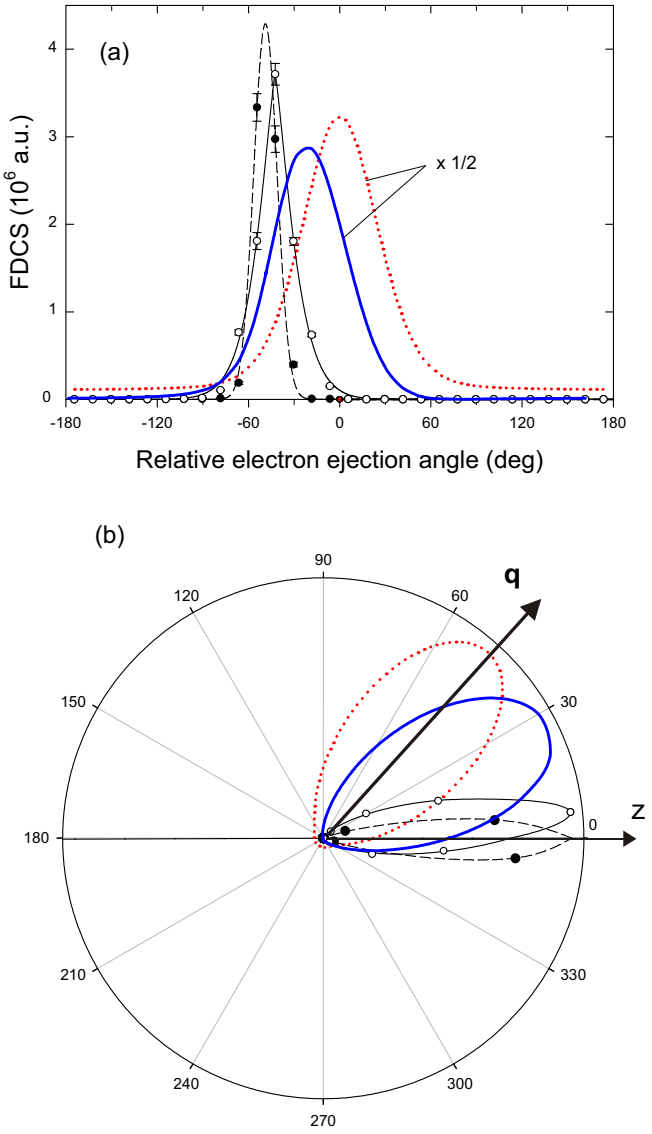

FIG. 2. (Color online) The same as Fig. 1 but for proton impact.

antiproton impact. Even without the NN interaction the obtained electron distribution is peaked at a backward angle, at $\theta_e \approx 120^\circ$ [see Fig. 1(b)]. Interestingly, the shape of this latter distribution is similar to that of the FBA: The two peaks have about the same width, but the distribution predicted by the CTMC method shows some asymmetry. This is in qualitative agreement with the TDCC results of Ciappina *et al.* [8] obtained without inclusion of the NN interaction. Concerning the peak intensities, the CTMC result is smaller by a factor of 3 than that of the FBA. The inclusion of the NN interaction led to a dramatic effect: The FDCS is further reduced by a factor of 5, and the angular distribution completely changed. In this case the electrons are emitted at even larger backward angles. The distribution has a maximum at $\theta_e \approx 220^\circ$, but a smaller peak is also visible at $\theta_e \approx 110^\circ$. A similar double-peak structure has been observed in quantum mechanical calculations [7–9]. In the latter works the smaller and the larger peak were identified as the binary and the recoil peak. In the following we refer to the two peaks using these notations.

A very different result was obtained for proton impact. Our calculations both without and with inclusion of the NN interaction show an opposite shift of the binary peak as compared to antiproton impact: The electrons are emitted at small angles in forward direction. The width of the distributions is much narrower than that predicted by the FBA. This indicates the presence of a strong two-center effect. The

intensity of the peaks is smaller than that predicted by the FBA, but the difference is smaller for protons than for antiprotons.

In Figs. 1 and 2 we plotted also FDCS data obtained from CDW-EIS calculations [15] without considering the NN interaction. The CDW-EIS model is also a perturbation theory like the FBA, but unlike the FBA it accounts for the distortion of the electronic states in the presence of the projectile. Therefore, the CDW-EIS model is expected to provide FDCS data that are closer to the CTMC results. Indeed, for antiproton impact the binary peak predicted by the CDW-EIS model is very similar to that obtained from the CTMC method, with regard to both its intensity and shape. At the same time, the CDW-EIS model predicts a smaller shift of the peak from the direction of q than does the CTMC method. The widths of the peaks also differ slightly; the CDW-EIS peak is broader. For proton impact the CDW-EIS model predicts a two-center effect much smaller than that predicted by the CTMC method; the CDW-EIS peak does not show the strong narrowing effect observed with the CTMC method.

In Figs. 3 and 4 we compare the present FDCS and doubly differential cross section (DDCS) results with those of quantum mechanical calculations. In Fig. 3 the quantum mechanical models used in the comparison are the TDCC theory of Ciappina *et al.* [8], the CCC approach of Abdurakhmanov *et al.* [7], and the CDW-EIS model of Voitkiv and Ullrich [9]. The FDCS data of the latter model were taken from Ref. [7]; we also made independent CDW-EIS calculations in the present work.

We note that the present CTMC data were evaluated in the laboratory reference system. At the same time, the published FDCS results of the above models were expressed in the *relative* coordinate system. To convert the latter data to the laboratory system we multiplied them by the factor $(m_p/\mu)^2$ (see, e.g., Ref. [14]), where μ_p is the reduced mass of the

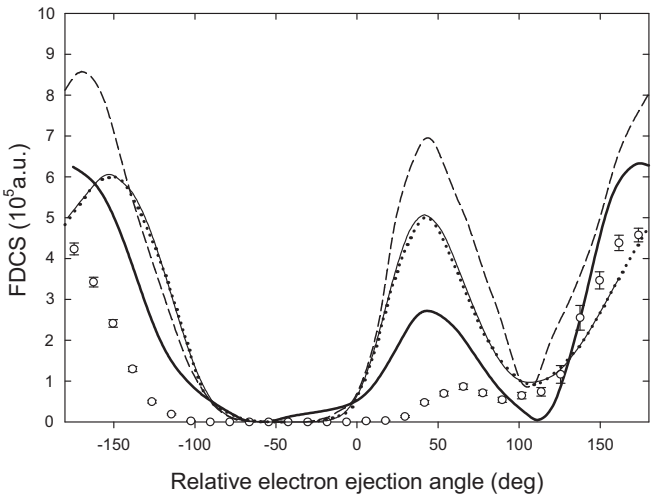

FIG. 3. Comparison of FDCS for antiproton impact obtained by the present CTMC calculations with the results of quantum mechanical models. All the calculations were made with inclusion of the NN interaction. Open circles with error bar, CTMC; thick solid line, TDCC [8]; dashed line, CCC [7]; dotted line, CDW-EIS [9]; thin solid line, CDW-EIS calculated in the present work.

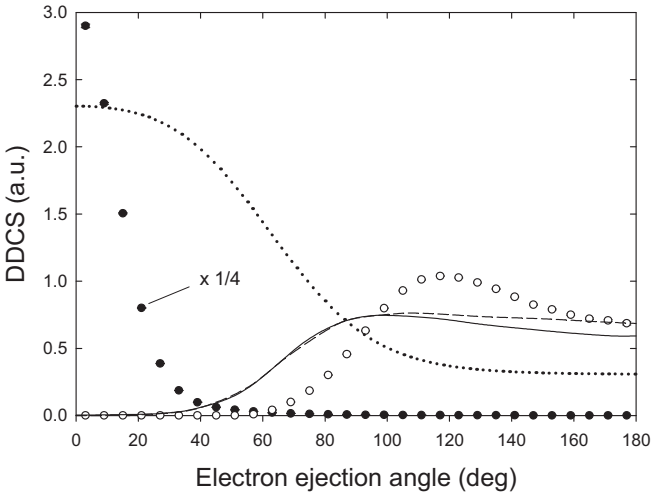

FIG. 4. DDCS for ejection of electrons of energy 5 eV as a function of the emission angle. The dotted line denotes the FBA. The present CTMC results are shown by open and solid circles for antiproton and proton impact, respectively. Quantum mechanical models for antiproton impact: solid line, CCC [7]; dashed line, CP [12].

projectile:

$$\mu_p = \frac{m_p m_H}{m_p + m_H}.$$

Here m_p and m_H are the mass of the projectile and that of the hydrogen atom, respectively. For proton (antiproton) on hydrogen scattering to a good approximation $(m_p/\mu)^2 \approx 4$. Unlike FDCS values, the DDCS values are the same in the two reference systems (due to the integration over θ_p); therefore we did not need to correct the DDCS data.

From Fig. 3 we can establish only qualitative agreement between the CTMC and the quantum mechanical models. The disagreement is particularly large for the binary peak concerning both its intensity and position. While all the three quantum mechanical models predict a peak position of about 45°, according to the CTMC model the peak appears at about 65°. The CTMC model predicts a greatly suppressed binary peak. For the recoil peak a better agreement is observed. In the latter case a striking feature of the CTMC results is the narrower peak width compared to other theories.

Concerning the greatly suppressed binary peak predicted by the CTMC method, we note that the description of this peak seems to be very sensitive to the the applied theoretical approach: Even for the quantum mechanical models the peak maximum varies by a factor of more than 2. Furthermore, we note that the CP calculations of McGovern *et al.* [14] carried out under identical collision conditions with the present work also resulted in a greatly suppressed binary peak relative to the recoil peak (see the three-dimensional plot of FDCSs in Fig. 1 of Ref. [14]).

There may be several reasons for the discrepancies between the CTMC and the quantum mechanical models. As is seen from Fig. 1, the inclusion of the NN interaction has a profound effect on the FDCS; therefore its approximate treatment may introduce uncertainties into the calculations.

As is discussed in the Introduction, the coupled-states descriptions (TDCC, CCC) are based on one-center expansion of the electronic wave function. This approximation is questionable at low impact energy [21]; thus the neglect of the two-center effects may be a further reason for the discrepancies. We note that in the CDW-EIS model the distortion factors applied at the initial- and final-state wave functions account for the two-center effect. However, the CDW-EIS model is a perturbation theory, and its use is justified at high impact energy.

As far as the CTMC model is concerned, it remains a question how far the FDCS is affected by the neglect of the quantum mechanical effects. Anyhow, the CTMC model seems to be suitable for the differential characterization of the antiproton-induced ionization of the hydrogen atom and may contribute in this way to a deeper understanding of the process.

In Fig. 4 the present DDCS results are compared with those of the CCC approach of Abdurakhmanov *et al.* [7] and the CP model of McGovern *et al.* [12] as a function of the electron emission angle. The energy of the electron is 5 eV. The CTMC data are plotted for both antiproton impact and proton impact and demonstrate well the expected large particle-antiparticle difference. The CTMC model predicts dominant electron emission at backward directions for antiproton impact, in qualitative agreement with the quantum mechanical models.

To investigate the role of the NN interaction in the antiproton-induced ionization, we analyzed particle trajectories under various collision conditions. As a great surprise, practically no difference was observed in the electron trajectories when the NN interaction was turned on and off. This is in contrast to the previous explanation of the NN interaction effect given by Abdurakhmanov *et al.* [7], who assumed an interference effect that takes place between the interactions of the target electron and proton with the outgoing antiproton. According to the authors, the outgoing scattered antiproton is decelerated in the attractive field of the target nucleus, resulting in a stronger final-state interaction between the antiproton and the electron. This leads to the polarization of the target electron cloud and a shift of the electron density away from the projectile path.

The insensitivity of the electron trajectories on the NN interaction observed in the present work indicates that the effect assumed by Abdurakhmanov *et al.* [7] is probably very small at the collision energies regarded also by the authors ($\geqslant$30 keV). Then the question is the following: How can one explain the drastic change in the FCDS seen in Fig. 1 when the NN interaction is turned on?

The answer was found by analyzing the trajectory of the target nucleus. We found that it changed to a large extent when the NN interaction was turned on. The change is caused by the momentum transferred by the projectile to the target nucleus in the NN scattering. As a result, the total momentum transferred to the whole atom is also changed, which leads to the rearrangement of the collision events and to a modified angular distribution.

The finding that the nucleon-nucleon scattering has practically no effect on the motion of the electron is understandable considering the very small scattering angle and the negligible change in collision velocity, as well as the length scale difference of 3 orders of magnitude between the motion of the electron and that of the target nucleus. The rigidity of

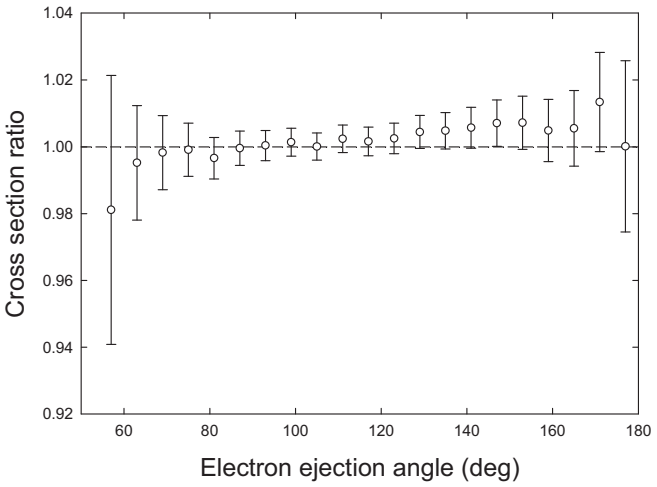

FIG. 5. Ratio of DDCS values calculated with inclusion of the NN interaction to those calculated without it. The energy of the ejected electron is 5 eV.

the angular distribution of the electron on the NN interaction is well reflected by the ratio of DDCS values for ejection of electrons of 5 eV calculated with and without the NN interaction. The ratio is plotted in Fig. 5 for electron ejection angles $\theta_e > 50^\circ$ at which DDCS takes appreciable values. Although systematical deviations from unity can be observed at smaller and larger angles, the effect is small ($<$2%) and within the error of the calculations.

Our finding that the relative motion between the electron and the nuclei is coupled very weakly with that between the nuclei indicates that two motions can be treated independently. This led us to show that the NN interaction can be be included in the calculations in the form of the following simple correction procedure. Let us denote the additional momentum transfer vector due to the NN scattering by $\mathbf{q}^{NN}$. For small scattering angles the longitudinal component of $\mathbf{q}^{NN}$ can be neglected, and the transversal component is given as

$$q_{\perp}^{\mathrm{NN}} \approx K_i\, \theta_p^{\mathrm{NN}}. \tag{6}$$

θ_p^{NN} is the NN two-body scattering angle that can be obtained from the relationship

$$\theta_p^{NN} = 2 \arctan\left(\frac{b}{a}\right), \tag{7}$$

where $a = Z_p Z_t / 2E_p$ is the half distance of closest approach (E_p is the energy of the projectile).

The correction procedure is simply the replacement of the momentum transfer vector $\mathbf{q}$ by the vector $\mathbf{q} + \mathbf{q}^{NN}$ for all the collision events that were calculated without the NN interaction. The FDCS data derived from the modified collision events are compared with those obtained with the "exact" treatment of the NN effect in Fig. 6. We may conclude from the figure that the correction procedure is excellent, thus proving the weak coupling between the electron-nuclei and the nucleon-nucleon relative motion. We note that the success of the presented approximate treatment of the NN effect gives strong support to the procedure applied by Schulz *et al.* [38] in the analysis of their experimental FDCS results obtained

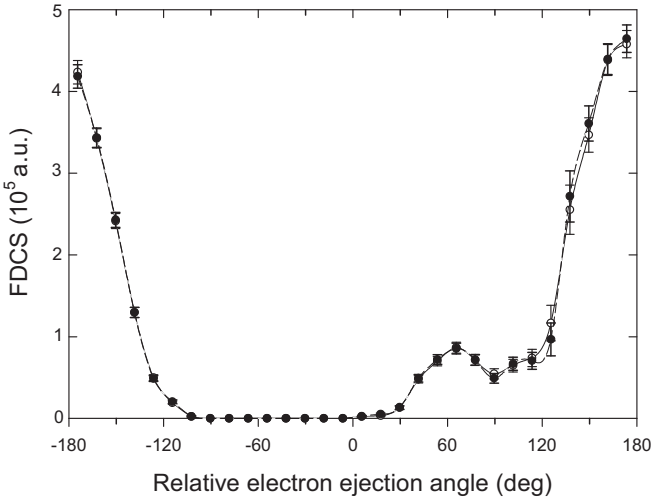

FIG. 6. Comparison of FDCS values obtained by approximate treatment of the NN interaction effect (solid circles) with the exact results (open circles).

for ionization in 100 MeV/amu C^{6+} + He collisions. The latter authors used the Monte Carlo event generator (MCEG) method in the FBA to account for the additional momentum transfer due to the elastic scattering of the projectile ion on the target nucleus. The application of the MCEG was necessary, because such a correction can be made only event-by-event, in such a way as it was done in our present CTMC investigation.

IV. CONCLUSIONS

We investigated the three-body dynamics of the ionization of the atomic hydrogen induced by antiprotons. To this end, we calculated FDCSs by applying the CTMC method. The calculations were made at the relatively low impact energy of 30 keV where large deviations from the predictions of the FBA are expected. The kinematical parameters (electron energy and projectile scattering angle) were chosen to be those of quantum mechanical investigations of the process available in the literature. The calculations also made for proton impact under the same collision conditions revealed large particle-antiparticle differences in FDCSs. Comparing the CTMC results with the predictions of quantum mechanical models (CCC, TDCC, CDW-EIS) we concluded that the classical mechanical description can reproduce the main features of the antiproton-induced ionization of the hydrogen atom, and thereby it helps the deeper understanding of the process. We analyzed the possible reasons for the observed discrepancies between the CTMC and the quantum mechanical models: the approximate treatment of the NN interaction and the use of the one-center expansion of the electronic wave function in the quantum mechanical descriptions on the one hand and the neglect of quantum effects in the CTMC model on the other hand.

To clarify the role of the NN interaction in ionization, we examined individual particle trajectories. We established that the relative motion between the electron and the nuclei is coupled very weakly with that between the nuclei; consequently the two motions can be treated independently. This was convincingly proven by a calculation in which the additional momentum transfer due to the elastic scattering of the projectile on the target nucleus was taken into account by a simple correction procedure for collision events obtained without inclusion of the NN interaction.

ACKNOWLEDGMENTS

This work was supported by the National Scientific Research Foundation (OTKA, Grant No. K109440) and the National Information Infrastructure Program (NIIF).

[1] T. Kirchner and H. Knudsen, J. Phys. B **44**, 122001 (2011).
[2] J. Ullrich, R. Moshammer, A. Dorn, L. Schmidt, and H. Schmidt-Böcking, Rep. Prog. Phys. **66**, 1463 (2003).
[3] Kh. Khayat *et al.*, J. Phys. B **32**, L73 (1999).
[4] M. R. F. Siggel-King, A. Papash, H. Knudsen, M. Holzscheiter, and C. P. Welsch, Hyperfine Interact. **199**, 311 (2011).
[5] M. Schulz, R. Moshammer, D. Fischer, H. Kollmus, D. H. Madison, S. Jones, and J. Ullrich, Nature (London) **422**, 48 (2003).
[6] K. A. Kouzakov, S. A. Zaytsev, Y. V. Popov, and Masahiko Takahashi, Phys. Rev. A **86**, 032710 (2012).
[7] I. B. Abdurakhmanov, A. S. Kadysrov, I. Bray, and A. T. Stelbovics, J. Phys. B **44**, 165203 (2011).
[8] M. F. Ciappina, T.-G. Lee, M. S. Pindzola, and J. Colgan, Phys. Rev. A **88**, 042714 (2013).
[9] A. B. Voitkiv and J. Ullrich, Phys. Rev. A **67**, 062703 (2003).
[10] S. Jones and D. H. Madison, Phys. Rev. A **65**, 052727 (2002).
[11] J. Berakdar, J. S. Briggs, and H. Klar, J. Phys. B **26**, 285 (1993).
[12] M. McGovern, D. Assafrão, J. R. Mohallem, C. T. Whelan, and H. R. J. Walters, Phys. Rev. A **79**, 042707 (2009).
[13] M. McGovern, D. Assafrão, J. R. Mohallem, C. T. Whelan, and H. R. J. Walters, Phys. Rev. A **81**, 032708 (2010).
[14] M. McGovern, D. Assafrão, J. R. Mohallem, C. T. Whelan, and H. R. J. Walters, J. Phys.: Conf. Series **212**, 012029 (2010).
[15] L. Gulyás, A. Igarashi, P. D. Fainstein, and T. Kirchner, J. Phys. B **41**, 025202 (2008).
[16] V. D. Rodríguez, J. Phys. B **29**, 275 (1996).
[17] B. Pons, Phys. Rev. A **63**, 012704 (2000).
[18] B. Pons, Phys. Rev. Lett. **84**, 4569 (2000).
[19] A. Igarashi, S. Nakazaki, and A. Ohsaki, Phys. Rev. A **61**, 062712 (2000).
[20] E. Y. Sidky and C. D. Lin, J. Phys. B **31**, 2949 (1998).
[21] N. Toshima, Phys. Rev. A **64**, 024701 (2001).
[22] L. Sarkadi, Phys. Rev. A **82**, 052710 (2010).
[23] G. W. Kerby III, M. W. Gealy, Y.-Y. Hsu, M. E. Rudd, D. R. Schultz, and C. O. Reinhold, Phys. Rev. A **51**, 2256 (1995).
[24] J. Fiol and R. E. Olson, Nucl. Instrum. Methods Phys. Res., Sect. B **205**, 474 (2003).

[25] M. Schulz *et al.*, J. Phys. B **34**, L305 (2001).
[26] L. Mengt, R. E. Olson, R. Dörner, J. Ullrich, and H. Schmidt-Böcking, J. Phys. B **26**, 3387 (1993).
[27] I. F. Barna, K. Tőkési, L. Gulyás, and J. Burgdörfer, Radiat. Phys. Chem. **76**, 495 (2007).
[28] K. Tőkési, J. Wang, L. Gulyás, and J. Burgdörfer, Hyperfine Interact. **194**, 45 (2009).
[29] R. Abrines and I. C. Percival, Proc. Phys. Soc., London **88**, 861 (1966).
[30] R. E. Olson and A. Salop, Phys. Rev. A **16**, 531 (1977).
[31] B. Sulik and K. Tőkési, Adv. Quantum Chem. **52**, 253 (2007).
[32] C. O. Reinhold and C. A. Falcón, Phys. Rev. A **33**, 3859 (1986).
[33] C. O. Reinhold and R. E. Olson, Phys. Rev. A **39**, 3861 (1989).
[34] L. Sarkadi and R. O. Barrachina, Phys. Rev. A **71**, 062712 (2005).
[35] H. Knudsen, U. Mikkelsen, K. Paludan, K. Kirsebom, S. P. Møller, E. Uggerhøj, J. Slevin, M. Charlton, and E. Morenzoni, Phys. Rev. Lett. **74**, 4627 (1995).
[36] M. B. Shah, D. S. Elliott, and H. B. Gilbody, J. Phys. B **20**, 2481 (1987).
[37] M. R. C. McDowell and J. P. Coleman, *Introduction to the Theory of Ion-Atom Collisions* (North-Holland, Amsterdam, London, 1970), p. 323.
[38] M. Schulz, M. Dürr, B. Najjari, R. Moshammer, and J. Ullrich, Phys. Rev. A **76**, 032712 (2007).